scientific reports

Check for updates

OPEN

Evaluation of the efficacy of P11-4 and CCP-ACPF in the prevention and treatment of white spot lesions: a multi-technique approach

Hikmetnur Danisman[1]✉, Ebru Delikan[1] & Kaan Orhan[2]

The aim of this study was to assess the efficacy of the self-assembling peptide P11-4 [Curodont Repair Fluoride Plus-self-assembling peptide (Curodont FP)] and casein phosphopeptide–amorphous calcium phosphate fluoride (CCP-ACPF) (MI Varnish) in the management of white spot lesions (WSLs), during orthodontic treatment. Eighty specimens were prepared from the buccal surfaces of bovine teeth and divided into five groups that received different treatment protocols with Curodont FP and MI Varnish. (1) MI- Pre-Post: MI varnish applied before and after demineralization; (2) MI-Post: MI varnish applied after demineralization; (3) Curodont- Pre-Post: Curodont FP applied before and after demineralization; (4) Curodont-Post: Curodont FP applied after demineralization; (5) Control: No remineralization agent applied after demineralization. MI Varnish was applied in a thin and uniform layer using a single-use brush. Before application of Curodont FP, the enamel surface was conditioned with 35% phosphoric acid, rinsed and gently air-dried, then applied with an applicator sponge. Generalized linear models and one-way ANOVA tests were used to analyze the data. The significance level was set at $p < 0.05$. Specimens were analyzed using micro-computed tomography (micro-CT), field-emission scanning electron microscopy (FE-SEM), and energy-dispersive X-ray spectroscopy (EDX). The lowest lesion depths after the 28-day period (T2) were observed in the MI-Pre-Post (0.14 mm), MI-Post (0.15 mm), and Curodont-Pre-Post (0.15 mm) groups ($p = 0.003$). The control group showed the lowest mineral density (2.28 gHA/cm^3), while the MI-Pre-Post, MI-Post, and Curodont-Pre-Post groups exhibited the highest mineral density (2.54 gHA/cm^3, 2.52 gHA/cm^3, 2.56 gHA/cm^3, respectively) and the lowest lesion depth. Lesion depth and mineral density notably improved over time, particularly after agent application. The application of MI varnish before orthodontic treatment protects the enamel against demineralization. MI Varnish and Curodont FP are highly effective for the remineralization of WSL and can be clinically preferred.

Keywords Demineralization, Fluoride varnish, Remineralization, Self-assembling peptide, White spot lesion, Micro-ct

Dental caries is one of the most prevalent adverse effects of fixed orthodontic treatment. Among the various forms of dental caries, white spot lesions (WSLs) are a particular concern and challenge for orthodontists. WSLs are defined as areas of demineralization on the enamel surface that exhibit a milky white and opaque appearance, progressing to the subsurface layer and serving as the initial clinical indicators of enamel caries[1]. The retention areas created by the fixed appliances during orthodontic treatment resulted in an increase in dental plaque volume. When this plaque, which has a lower pH than non-orthodontic patients, is accompanied by poor oral hygiene, the risk of WSL formation is significantly elevated[2]. The lower pH of the plaque, coupled with variations in plaque composition and an increased prevalence of S. mutans within the plaque, further contributes to the increased incidence of WSL formation[3,4]. It has been reported that very shallow initial lesions can be detected on the enamel surface within two weeks of plaque formation and the onset of demineralization[5]. As the demineralization process progresses, there is an increased risk of these lesions transitioning to cavitation[6]. A multitude of studies in the literature have reported an increased incidence of WSL formation during fixed orthodontic treatment, particularly in patients with poor oral hygiene, with rates ranging from 23.4 to 75.6%[7,8].

[1]Department of Orthodontics, School of Dentistry, University of Nuh Naci Yazgan, Kayseri, Turkey. [2]Department of Oral and Maxillofacial Radiology, School of Dentistry, University of Ankara, Ankara, Turkey. ✉email: hnurdanisman@gmail.com

One of the main goals of orthodontic treatment is to improve smile aesthetics. However, in contrast to this purpose, WSLs are a factor that leads to the deterioration of aesthetic appearance. The potential for WSL to progress to advanced cavitation, combined with its detrimental effect on aesthetic appearance, necessitates both their treatment and, more importantly, their prevention in the first place. To prevent the formation of WSL, good oral hygiene, a diet low in carbohydrates, and the use of oral care products containing fluoride are recommended. Many noninvasive preventive strategies have been proposed to reduce enamel demineralization and facilitate the remineralization process. Various remineralization agents are currently used to treat WSL. The use of fluoride for enamel remineralization continues to be widely accepted as the gold standard for preventing dental caries[9]. Fluoride, known primarily for its anticariogenic effects, hardens the mineral surface layer and inhibits the progression of WSLs, thereby inactivating caries[10]. Among fluoride application methods, fluoride varnish is a frequently preferred method in the treatment of WSL because it is less dependent on patient compliance[11]. Hovewer, fluoride has a high affinity for hydroxyapatite; it becomes trapped on the demineralized surface and cannot penetrate the subsurface demineralized region[12]. In these conditions, adequate remineralization may not be achieved in deep lesions.

Casein phosphopeptide-amorphous calcium phosphate (CPP-ACP) is a bioactive agent formulated from casein phosphopeptides (CPP), which are found in milk and dairy products, and amorphous calcium phosphate (ACP) complexes[13]. The application of agents containing CPP-ACP has been shown to facilitate subsurface remineralization in initial enamel caries. This is achieved through the provision of a reservoir for calcium and phosphate ions, buffering of acidic pH to promote hydroxyapatite formation, and elevation of oral pH through enhancement of calcium salt solubility[14]. The combination of CPP-ACP with external fluoride ions, such as casein phosphopeptide-amorphous calcium fluoride phosphate (CPP-ACPF), which is predicted to make the remineralization process more effective by providing long-term stabilization of calcium and phosphate ions on demineralized enamel surfaces, has been launched in various products[15]. According to the study of Llena et al.[16] evaluating the effects of CPP-ACP, CPP-ACPF, and 5% sodium fluoride (NaF) varnish on early carious lesions, CPP-ACPF was found to be more effective in reducing early carious lesions than the other two agents. However, although CPP-ACP is a dairy product, it cannot be administered to patients with milk intolerance. In addition, its success in remineralization with fluoride agents has been controversial in the literature[15,17–20]. Consequently, novel strategies have been devised to overcome these limitations.

A novel protective approach, self-assembling peptide P11-4 (SAP P11-4), has been developed recently in response to the discovery of enamel matrix proteins, with the aim of enhancing enamel remineralization[5,12,21]. Self-peptide technology is based on the Guided Enamel Regeneration (GER) technology, which is based on the creation of a scaffold that mimics the enamel matrix[5]. The aim of self-peptide technology is to facilitate the remineralization of subsurface lesions by creating a scaffold consisting of a 3D hydrophilic peptide[9]. This biomimetic scaffold is capable of nucleating hydroxyapatite. The anionic groups present in the SAP P11-4 side chains attract calcium ions, causing the calcium phosphate salts to precipitate hierarchically on the preformed scaffold. It has been reported that self-peptides, which also have a high affinity for calcium ions in saliva, act as biomimetics and provide a remineralization effect by enabling the deposition and growth of hydroxyapatite crystals on the enamel[12,21–23]. The addition of NaF to SAP P11-4 aims to enhance remineralization more rapidly through a synergistic effect while preserving all previously noted benefits[24].

A growing body of literature supports the therapeutic role of fluoride varnishes and self-peptides on enamel surfaces. However, to the best of our knowledge, no study in the literature has simultaneously evaluated both the preventive and therapeutic efficacy of these agents while also employing multiple imaging techniques to assess this efficacy. In light of the aforementioned facts, the primary objective of this study was to evaluate the potential of SAP P11-4 and CPP-ACPF based varnish as demineralization inhibitors in intact tooth enamel. The secondary objective was to assess the effectiveness of these two agents in promoting enamel remineralization. The efficacy of SAP P11-4 with fluoride- and CPP-ACPF-based varnish was evaluated using a range of analytical techniques, including micro-computed tomography (micro-CT), field-emission scanning electron microscopy (FE-SEM), and energy-dispersive X-ray spectroscopy (EDX). The null hypothesis was that the application of CPP-ACPF-based varnish and SAP P11-4 would not prevent enamel demineralization or improve the remineralization process of WSL.

Methods

The study protocol was approved by the Ethical Committee of Nuh Naci Yazgan University (reference number: 2023/003–004). In this study, the efficacy of two different remineralization agents, CPP-ACPF-based varnish containing 5% CPP-ACP and 22,600 ppm fluoride [MI Varnish (MI Varnish; GC, Tokyo, Japan)] and SAP P11-4 containing 0.05% NaF [Curodont FP (Curodont Repair Flouride Plus; vVardis, Switzerland)] on artificial dental caries was investigated using different protocols. The chemical compositions, types, manufacturers, batch numbers and fluoride concentrations of the remineralization agents are listed in Table 1. Figure 1 presents a schematic diagram of the study design.

Specimen preparation

The sample size was determined by power analysis using the G-Power package program (version 3.1.9.4, Heinrich Heine University of Düsseldorf, Düsseldorf, Germany). Based on one-way analysis of variance with 95% confidence (1-α), 80% test power (1-β), and an effect size of f = 0.40, the number of specimens required for the study was determined to be 80, with 16 specimens in each group (Group 1–5) for micro-CT analysis[25]. A further four specimens were added for EDX analysis of the mineral content of the sound enamel, resulting in a total of 84 specimen requirements.

Eighty bovine incisors were obtained from freshly slaughtered cattle in accordance with relevant guidelines and regulations. The study is reported in accordance with the ARRIVE guidelines. The buccal surfaces of the

Trade name	Main components	Type	Manufacturer	Batch number	Fluoride concentration (ppm)
MI Varnish	Sodium Fluoride 0.05%, phosphate-amorphous-casein with calcium phosphate (Recaldent-CPP-ACP)	Varnish	GC, Tokyo, Japan	220623 A	22,600
Curodont Repair Flouride Plus	Inactive ingredients: Water, Chlorhexidine Digluconate, Tromethamıne, Trehalose Dihydrate, Oligopeptide-104, Hydroxypropyl Methylcellulose Active ingredients: Sodium Fluoride 0.05% (0.02% W/V Fluoride Ion)	Brush-on system	vVARDIS, Switzerland	CH220252-882	500

Table 1. Trade names, main components, types, manufacturers, fluoride concentration of the tested remineralization agents.

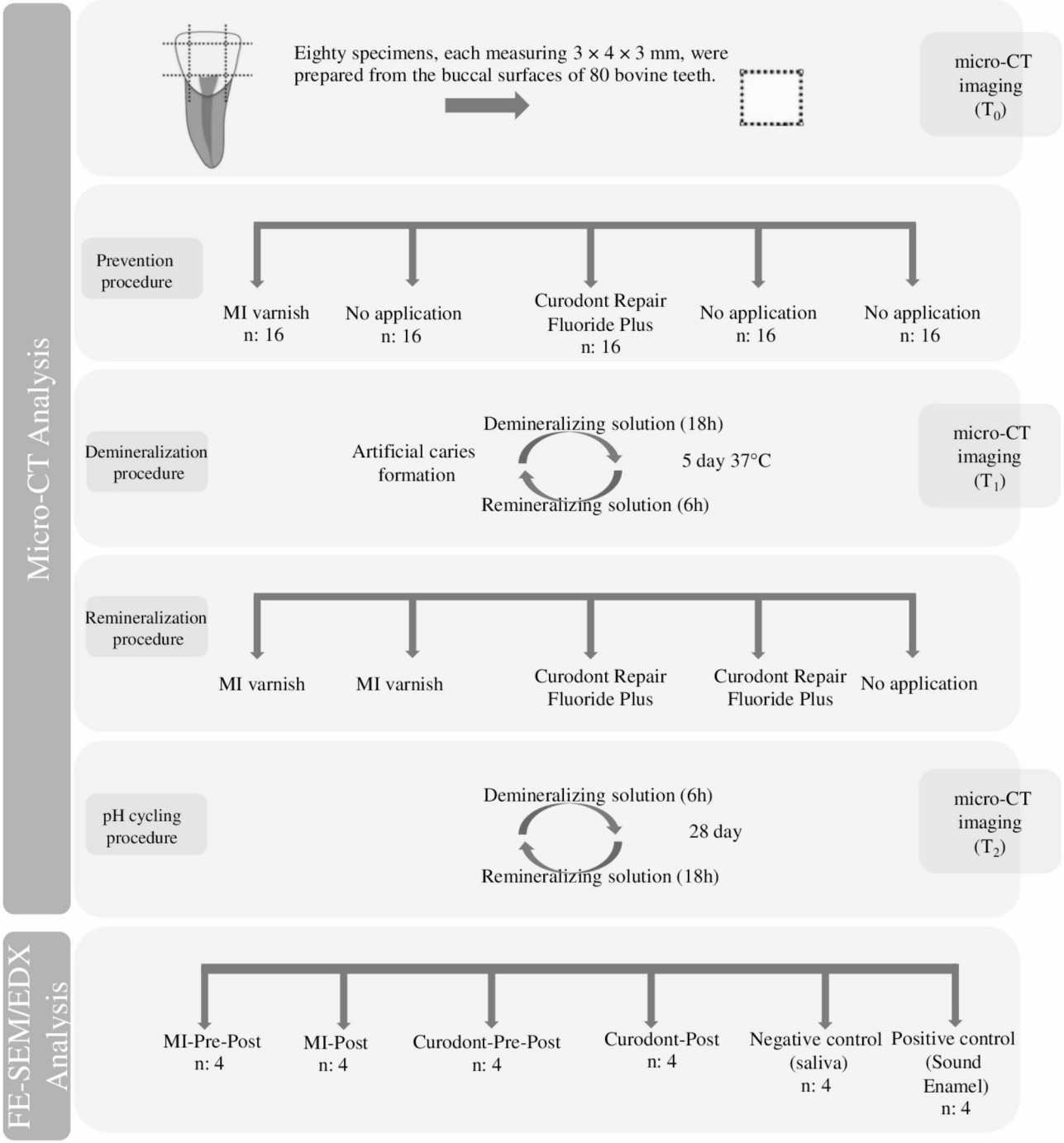

Fig. 1. Schematic diagram of the study design.

teeth were examined using a dental microscope (OMS2350; ZUMAX, Jiangsu, China) to identify and exclude any surface defects such as hypoplastic areas or cracks. Any defective ones were replaced with new ones that met the required standards. Residual soft tissues and periodontal fibers on the root surface were meticulously removed using a scaler (Hu–Friedy Mfg. Co., Chicago, USA). Afterward, the teeth were polished with a slurry of pumice and stored in 0.5% chloramine-T bacteriostatic solution (Merck, Darmstadt, Germany). The storage solution was refreshed weekly until the experimental procedures were commenced.

Subsequently, the roots were removed at the cementoenamel junction using a precision cutter (Microcut 201; Metkon; Bursa, Türkiye). The crowns were then bisected in the coronoincisal direction with a high-speed water-cooled diamond-coated disc (Frank Dental, Germany), producing 80 rectangular enamel block specimens, approximately 3 × 4 × 3 mm in size, from the buccal surfaces of each crown under water cooling.

The specimens were selected by a simple random method without replacement using online randomization software (version 4, https://randomizer.org/) and were divided into five groups ($n = 16$) based on the remineralization agents and the treatment strategy to be applied:

1. *MI-Pre-Post*: MI varnish applied before and after demineralization.
2. *MI-Post*: MI varnish applied after demineralization.
3. *Curodont- Pre-Post*: Curodont FP applied before and after demineralization.
4. *Curodont-Post*: Curodont FP applied after demineralization.
5. *Control*: No remineralization agent applied after demineralization (negative control group, stored in saliva).

The specimens were embedded in acrylic blocks to expose the buccal enamel surface. Baseline micro-CT imaging (T0) of each specimen was performed to measure the mineral density of intact enamel.

Subsequently, the buccal surfaces of the specimens in the MI-Pre-Post were dried, and a thin, uniform layer of MI Varnish was applied using its own single-use brush, following the manufacturer's instructions to ensure a standardized application. The varnish was stirred with a brush before application, and only a single layer was applied to minimize clumping. The teeth remained intact for 4 h according to the manufacturer's instructions. For the specimens in Curodont- Pre-Post, the buccal surfaces were cleaned using a small cotton pellet dipped in 2-3% sodium hypochlorite for 20 s, rinsed with water, and dried. After applying 35% phosphoric acid to the surface for 20 s, it was rinsed and slightly dried. The Curodont FP applicator sponge (containing a standard-volume agent) was then removed and pressed against the enamel surface to squeeze out all fluids. In accordance with the manufacturer's instructions, the solution was left in place for 35 min (5 min + 30 min). For the MI-Post, Curodont-Post, and control groups, no pretreatment was performed before the demineralization procedure.

Demineralization procedure

Each specimen was placed in amber-colored glass vials and was then exposed to a pH cycling procedure for 5 days at 37 °C according to the method described by Vieira et al.[26] They were subjected daily to replenished immersion in a demineralizing solution [pH = 5, 3 m*M* $CaCl_2$. $2H_2O$, 3 m*M* KH_2PO_4, 50 m*M* CH_3COOH, 10 *M* KOH, 2–50 µ*M* methylhydroxydiphosphonic acid (MHDP)][27] for 18 h and in a remineralizing solution (artificial saliva) (KH_2PO_4, Na_2HPO_4, KCL, NaSCN, NaCL, CaCl, NH_4Cl, urea, glucose, ascorbic acid, mucin, in 1000 ml distilled water, pH = 6,4)[28] for 6 h to create an artificial carious lesion. After completing the procedure, the specimens were rinsed with distilled water for 10 s to remove any remaining solution, and air-dried. They were then examined microscopically to verify the presence of a dull, whitish surface, characteristic of typical early enamel lesions.

Following the demineralization process, micro-CT imaging was conducted again (T1) to assess the lesion depth, volume, surface area, and mineral density.

Remineralization procedure

Following the same procedures as initially, MI Varnish was reapplied to the specimens in the MI-Pre-Post, while Curodont FP was reapplied to the specimens in the Curodont-Pre-Post. MI Varnish was applied to the specimens in the MI-Post, and Curodont FP was applied to the specimens in the Curodont-Post for the first time, adhering to the same protocols.

pH cycling procedure

Over a period of 28 d at 37 °C, all specimens in the five groups underwent a pH cycling process to simulate the pH changes occurring in the oral cavity, alternating between demineralization and remineralization solutions. Each cycle consisted of 6 h of demineralization followed by 18 h of remineralization[29]. The solutions were renewed at the beginning of each cycle and the specimens were briefly rinsed with distilled water to remove any residual solution. After the 28-day experimental period, a third round of micro-CT imaging (T2) and SEM analysis were conducted.

Micro-CT analysis

A high-resolution desktop micro-CT system (Skyscan 1275, Skyscan, Kontich, Belgium) was used to scan the specimens. The scanning conditions were 80 kVp, 125-mA beam current, 0.5-mm Al/Cu filter, 15.2-µm pixel size, rotation at 0.5 step, and beam hardening of 40%. To minimize ring artifacts, air calibration of the detector was performed prior to each scan. Each sample was rotated by 360° within an integration time of 5 min. The mean scanning time was approximately 2 h. Other settings included a beam-hardening correction and input of optimal contrast limits (0-0.0005), based on prior scanning and reconstruction of the teeth.

The Nrecon software (ver. 1.7.1.2; Skyscan, Kontich, Belgium) and CtAn (ver. 1.15.1, Skyscan) were used for visualization and quantitative measurements of the specimens, using a modified version of the algorithm

described by Feldkamp et al.[30] to obtain axial two-dimensional, 1000 × 1000-pixel images. For the reconstruction parameters, the ring artifact correction and smoothing were fixed at zero, and the beam artifact correction was set at 40%. Contrast limits were applied following SkyScan instructions. A similar procedure was used to measure the gray values of the two mineral density phantom rods. To aid mineral density (MD) calculations, greyscale values were converted into MD values (gHAp cm^{-3}) with a linear calibration curve based on the greyscale values obtained from the two mineral concentration conical phantoms of 0.25 and 0.75 gHAp cm^{-3}. A region of interest (ROI) was chosen 2 × 2 mm around the enamel defects. The enamel mineral loss difference (ΔZ; gHAp cm^{-3}) of each specimen was calculated in the ROI by calculating the MD values from the entire demineralized enamel area as a mean of loss of surface and inner part of the demineralized enamel area. Enamel mineral loss was defined after subtracting the demineralized MD values from the baseline phantom rod MD values to correct the alignment inaccuracies from the specimen.

Lesion depth (LD) was calculated by subtracting the area of demineralization from the area of the sound enamel in the same ROI. Three calculations were performed for each tooth area and the average result was calculated as the final LD. The LD difference (ΔLD; mm) was calculated by subtracting the demineralized LD values in each group from the baseline LD values. Measurements were performed from the demineralized area on the tooth surface to the last point of the demineralized area, and some procedures were performed after remineralization. Lesion volume (mm^3) and lesion surface area (mm^2) were also calculated after demineralization and remineralization.

The reconstructed images, which were further processed using the Skyscan CTVox (ver. 3.3.0, SkyScan) for visualization (Skyscan, Kontich, Belgium). All reconstructions were made using a.3-inch flat-panel color-active matrix TFT medical display (NEC MultiSync MD215MG, Munich, Germany) with a resolution of 2048–2560 at 75 Hz and a 0.17-mm dot pitch operated at 12 bits.

FE-SEM-EDX analysis

Four randomly selected specimens from each of the five groups were prepared by removing the enamel surfaces from acrylic blocks. In addition, four specimens with the same dimensions were prepared for SEM and EDX analyses to examine the sound enamel. The specimens were ultrasonically washed thrice with distilled water, dehydrated in a series of ethanol solutions, and then dehydrated in a desiccator. A total of 24 specimens were mounted on metal stubs with the enamel surface facing upward using carbon tape. The specimens were subsequently sputter coated with Au/Pd (80%-20%) using a vacuum coater. Surface topographies were analyzed at magnifications of 500x and 10,000 × using a field-emission scanning electron microscope (FE-SEM, Gemini 500, Zeiss, Oberkochen, Germany) operating at an accelerating voltage of 20 kV.

EDX was used to analyze the Ca and P compositions of the specimen surfaces. Elemental analysis was conducted by integrating a secondary electron detector (EDAX Octane Elect, Amatek, USA) with the FE-SEM. The detector parameters included a sensitivity level of 0.5% (by weight), resolution of 133 eV, amplification time of 100 µs, and measurement duration of 60 s. The standard imaging resolution was set at 1536 × 1024 pixels. EDX-SEM microanalyses were performed at 500× magnification in three randomly selected fields, each measuring 50 µm × 50 µm, on each specimen. Elemental microanalysis employed the ZAF correction method, which separately calculates the effects of the atomic number (Z), absorption (A), and fluorescence (F) spatially and pointwise. The analysis yielded graphical and tabular representations of the elemental content and concentration within the examined areas.

Statistical analysis

Statistical analyses were performed using Statistical Package for the Social Sciences (ver. 29.0.2.0, SPSS Inc., Chicago, IL, USA). The normality of the data was assessed using the Shapiro-Wilk test, and skewness and kurtosis values were examined. Generalized linear models (GLMs) was used to determine the depth, volume, area, and mineral density of the enamel according to the application groups and different time periods. One-way ANOVA was conducted to assess the differences in elemental composition values, followed by multiple comparisons using Tukey's test. The results are presented as the mean ± standard deviation. The significance level was set at $p < 0.050$.

Results

Assessment of micro-CT analysis

Lesion depth

The mean lesion depth and standard deviation values for the groups and periods are shown in Table 2. The main effect of group on lesion depth was significant ($p = 0.003$). Mean lesion depth scores were 0.19 mm in the MI-Pre-Post, MI-Post, 0.20 mm in Curodont-Pre-Post, 0.22 in Curodont-Post, and 0.21 in control. The lowest lesion depths, with no significant differences among them, were observed in the MI-Pre-Post, MI-Post, and Curodont-Pre-Post. Conversely, the mean lesion depth values in the Curodont-Post and control groups were significantly higher than those in the first three groups. The main effect of time was also statistically significant ($p < 0.001$), with the total mean lesion depth value decreasing from 0.25 mm at T1 (post-demineralization) to 0.16 mm at T2 (28 days post-administration of remineralization agents). The interaction between the group and time was statistically significant ($p < 0.001$). At T2, there was no difference among MI-Pre-Post, MI-Post, and Curodont-Pre-Post, which exhibited the lowest mean lesion depth values. The multiple comparison results are presented in Table 2.

Lesion volume

The mean lesion volumes and standard deviation values for the groups and periods are shown in Table 2. The main effect of group on lesion volume values was not significant ($p = 0.439$), with mean lesion volume values

	Time		Total	Test statistics		p
	T1	T2				
Lesion depth (mm)						
MI-Pre-Post	0.25 ± 0.041^{a}	0.14 ± 0.031^{b}	0.19 ± 0.062^{AE}	Group	15.882	**0.003**
MI-Post	0.23 ± 0.033^{a}	0.15 ± 0.026^{be}	0.19 ± 0.052^{E}	Time	165.711	**< 0.001**
Curodont- pre-post	0.25 ± 0.055^{a}	0.15 ± 0.027^{be}	0.20 ± 0.068^{AE}	Group x Time	25.745	**< 0.001**
Curodont- post	0.28 ± 0.053^{c}	0.17 ± 0.044^{e}	0.22 ± 0.070^{BC}			
Control	0.22 ± 0.034^{a}	0.20 ± 0.054^{de}	0.21 ± 0.045^{AC}			
Total	0.25 ± 0.047	0.16 ± 0.043	0.20 ± 0.061			
Lesion volume(mm^3)						
MI-Pre-Post	0.27 ± 0.098	0.16 ± 0.065	0.22 ± 0.100	Group	3.764	0.439
MI-Post	0.24 ± 0.080	0.22 ± 0.183	0.23 ± 0.139	Time	15.733	**< 0.001**
Curodont- Pre-Post	0.23 ± 0.125	0.15 ± 0.086	0.19 ± 0.112	Group x Time	3.977	0.409
Curodont- Post	0.23 ± 0.097	0.18 ± 0.069	0.20 ± 0.087			
Control	0.25 ± 0.092	0.20 ± 0.055	0.22 ± 0.079			
Total	0.24 ± 0.099	0.18 ± 0.103	0.21 ± 0.105			
Lesion area(mm^2)						
MI-Pre-Post	1.38 ± 0.173	1.17 ± 0.162	1.27 ± 0.198	Group	2.683	0.612
MI-Post	1.37 ± 0.137	1.13 ± 0.165	1.25 ± 0.192	Time	85.606	**< 0.001**
Curodont- Pre-Post	1.35 ± 0.126	1.15 ± 0.165	1.25 ± 0.178	Group x Time	2.063	0.724
Curodont- Post	1.35 ± 0.095	1.08 ± 0.131	1.22 ± 0.175			
Control	1.31 ± 0.165	1.15 ± 0.184	1.23 ± 0.191			
Total	1.35 ± 0.140	1.14 ± 0.161	1.24 ± 0.185			

Table 2. Investigation of the effect of group and time on mineral density values. Note: Depth, volume and area values are based on the the Generalized linear models (GLMs) test; a-g No difference between interactions with the same letter, A-E No difference between main effects with the same letter, p-values presented in bold font indicate statistical significance ($p < 0.05$).Abbreviations: MI-Pre-Post: MI varnish applied before and after demineralization, MI-Post: MI varnish applied after demineralization, Curodont-Pre-Post: Curodont FP applied before and after demineralization, Curodont-Post: Curodont FP applied after demineralization, Control: No remineralization agent applied after demineralization (kept in saliva), *T1* Micro-CT imaging following demineralization, *T2* Micro-CT imaging after experimental period (28 days)

ranging from 0.19 mm^3 to 0.23 mm^3. However, the main effect of time was significant ($p < 0.001$), with the total mean lesion volume decreasing from 0.24 mm^3 at T1 to 0.18 mm^3 at T2. The interaction between the group and time was not statistically significant ($p = 0.409$). Additional multiple comparison results for the lesion volume are presented in Table 2.

Lesion area

The mean lesion area and standard deviation values for the groups and periods are shown in Table 2. The main effect of group on lesion area was not significant ($p = 0.612$). The lesion area values were as follows: MI-Pre-Post had a value of 1.27 mm^2, MI-Post and Curodont-Pre-Post had values of 1.25 mm^2, Curodont-Post had a value of 1.22 mm^2, and control group had a value of 1.23 mm^2. In contrast, the main effect of time on lesion area values was statistically significant ($p < 0.001$), with the total mean lesion area value decreasing from 1.35 mm^2, at T1 to 1.14 mm^2, at T2. The interaction between group and time did not have a significant effect on the lesion area values ($p = 0.724$). At T2, the groups exhibited similar mean lesion areas. The multiple comparison results for the lesion area are detailed in Table 2.

Mineral density

The mean mineral density and standard deviation values for the groups and periods are listed in Table 3. The micro-CT images obtained from one sample of each group are shown in Fig. 2. The main effect of group on mineral density was significant ($p < 0.001$). The highest mean mineral density values were observed in the MI-Pre-Post (2.56 gHA/cm^3), MI-Post (2.55 gHA/cm^3), and Curodont-Pre-Post (2.53 gHA/cm^3). The lowest mean mineral density value was detected in the control group (2.44 gHA/cm^3), which was significantly lower than that in the other groups. The main effect of time on mineral density was statistically significant ($p < 0.001$). The total mineral density values at T0, T1, and T2 were 2.77 gHA/cm^3, 2.28 gHA/cm^3, and 2.48 gHA/cm^3, respectively. The lowest total mean mineral density was found in T1, whereas the highest was found in T0. Additionally, the interaction between the group and time was statistically significant ($p < 0.001$). At T0, similar mineral density values were observed across all groups, whereas at T1, the mineral density values in MI-Pre-Post and MI-Post were significantly higher than those in the other three groups. At T2, the mineral density in the control group was significantly lower than that in all other groups. At T0, T1, and T2, a significant decrease in mineral density was observed from T0 to T1 across all groups. From T1 to T2, a significant increase in mineral density was noted

	Time			Total		Test statistics	*p*
	T0	T1	T2				
Mineral density(gHA/cm^3)							
MI-Pre-Post	2.76 ± 0.006^{c}	2.33 ± 0.103^{a}	2.54 ± 0.137^{b}	2.56 ± 0.208^{A}	Group	82.16	**< 0.001**
MI-Post	2.78 ± 0.008^{c}	2.34 ± 0.139^{a}	2.52 ± 0.114^{b}	2.55 ± 0.207^{A}	Time	1830.61	**< 0.001**
Curodont- Pre-Post	2.79 ± 0.007^{c}	2.24 ± 0.045^{d}	2.56 ± 0.098^{b}	2.53 ± 0.231^{AE}	Group x Time	110.277	**< 0.001**
Curodont- Post	2.75 ± 0.005^{c}	2.24 ± 0.033^{d}	2.52 ± 0.108^{b}	2.51 ± 0.233^{BE}			
Control	2.78 ± 0.007^{c}	2.24 ± 0.033^{d}	2.28 ± 0.029^{d}	2.44 ± 0.251^{C}			
Total	2.77 ± 0.007^{A}	2.28 ± 0.094^{B}	2.48 ± 0.146^{C}	2.51 ± 0.229			

Table 3. Investigation of the effect of group and time on mineral density values Mineral density values are based on the the Generalized linear models (GLMs) test; a-d No difference between interactions with the same letter, A-E No difference between main effects with the same letter, p-values presented in bold font indicate statistical significance (p<0.05). *MI-Pre-Post* MI varnish applied before and after demineralization, *MI-Post* MI varnish applied after demineralization, *Curodont-Pre-Post* Curodont FP applied before and after demineralization,*Curodont-Post* Curodont FP applied after demineralization, *Control* No remineralization agent applied after demineralization (kept in saliva), *T0* baseline micro-CT imaging, *T1* Micro-CT imaging following demineralization, *T2* Micro-CT imaging after experimental period (28 days)

in all groups, except the control group. The multiple comparison results for mineral density are presented in Table 3.

FE-SEM and EDX analysis

SEM images of the sound enamel and experimental specimen surfaces (after the 28-day period) are shown in Fig. 3. Upon evaluation of the SEM micrographs at 500X (a1, b1, c1, d1, e1, f1) and 10,000 × (a2, b2, c2, d2, e2, f2) magnifications, CaF_2 precipitation on the demineralized regions of MI-Pre-Post (a1 and a2) and MI-Post (b1 and b2) was observed. The most similar SEM images of the sound enamel (f1 and f2) were observed in these two groups. Additionally, in Curodont-Pre-Post (c1 and c2) and Curodont-Post (d1 and d2), guided enamel repair characterized by the induction of fiber formation (indicated by white arrows) on demineralized enamel and the development of a three-dimensional matrix was identified. Notably, MI-Pre-Post and Curodont-Pre-Post exhibited more pronounced mineral precipitation (images a2 and c2) than MI-Post and Curodont-Post (images b2 and d2). The 500X magnification SEM images of the control group (e1 and e2) revealed a honeycomb structure of demineralized enamel, whereas the dissolved centers of enamel prisms (marked by black arrows) were clearly visible in the 10,000 × SEM image.

The mean elemental Ca and P content values (%) and their respective standard deviations for the groups and the sound enamel are presented in Table 4. Analysis of the effects of the experimental remineralization agents on the enamel surface Ca and P composition revealed that the remineralization agent in the MI-Pre-Post significantly increased the enamel surface Ca ratio compared to the control group ($p = 0.040$). Similarly, the remineralization agent in MI-Pre-Post significantly increased the enamel surface P ratio compared to that in Curodont-Pre-Post and Curodont-Post ($p < 0.001$). The Ca and P values for each experimental group were comparable (with no statistically significant differences) to those of the sound enamel group. The Ca/P ratio in Curodont-Pre-Post and Curodont-Post was similar to that of MI-Pre-Post; however, it was significantly higher than that in the other groups and sound enamel. In contrast, the MI-Post and control groups exhibited a Ca/P ratio comparable to that of the sound enamel.

Discussion

White spot lesions (WSLs) are a common side effect of fixed orthodontic treatment, underscoring the need for effective remineralization strategies. Inconsistencies in the literature regarding demineralization inhibition and remineralization potential require further research. This study aimed to evaluate the efficacy of self-assembling peptides and fluoride varnishes on remineralization and their potential in preventing demineralization using micro-CT analysis. The results of this in vitro study indicate that MI Varnish is more effective in preventing demineralization than Curodont FP, and that both agents exhibit superior remineralization capacity compared to the negative control group. Therefore, the null hypothesis was rejected.

To evaluate the protective effects of agents with potential cariostatic properties against enamel demineralization, two remineralization agents were applied to sound enamel, followed by exposure to pH cycling. The results indicate that the reduction in mineral density was greater in the Curodont FP-treated specimens than in the MI varnish, with no significant difference observed between the Curodont FP group and the negative control. This suggests that MI Varnish may be more effective than Curodont FP in preventing demineralization. Literature on the protective effects of self-assembling peptides is limited and presents varying outcomes, underscoring the need for further investigation in this area[29,31]. Yaşar et al. used a pH-cycled demineralization model and found that the peptide (MMP3) showed a protective effect similar to that of the control group, similar to our study[29]. In a study by Takahashi et al., it was reported that SEM images of samples treated with Curodont Repair after undergoing a demineralization protocol exhibited smoother surfaces and less demineralization than those that did not receive the treatment[31]. Differing to our study, which utilized micro-CT for more precise mineral density

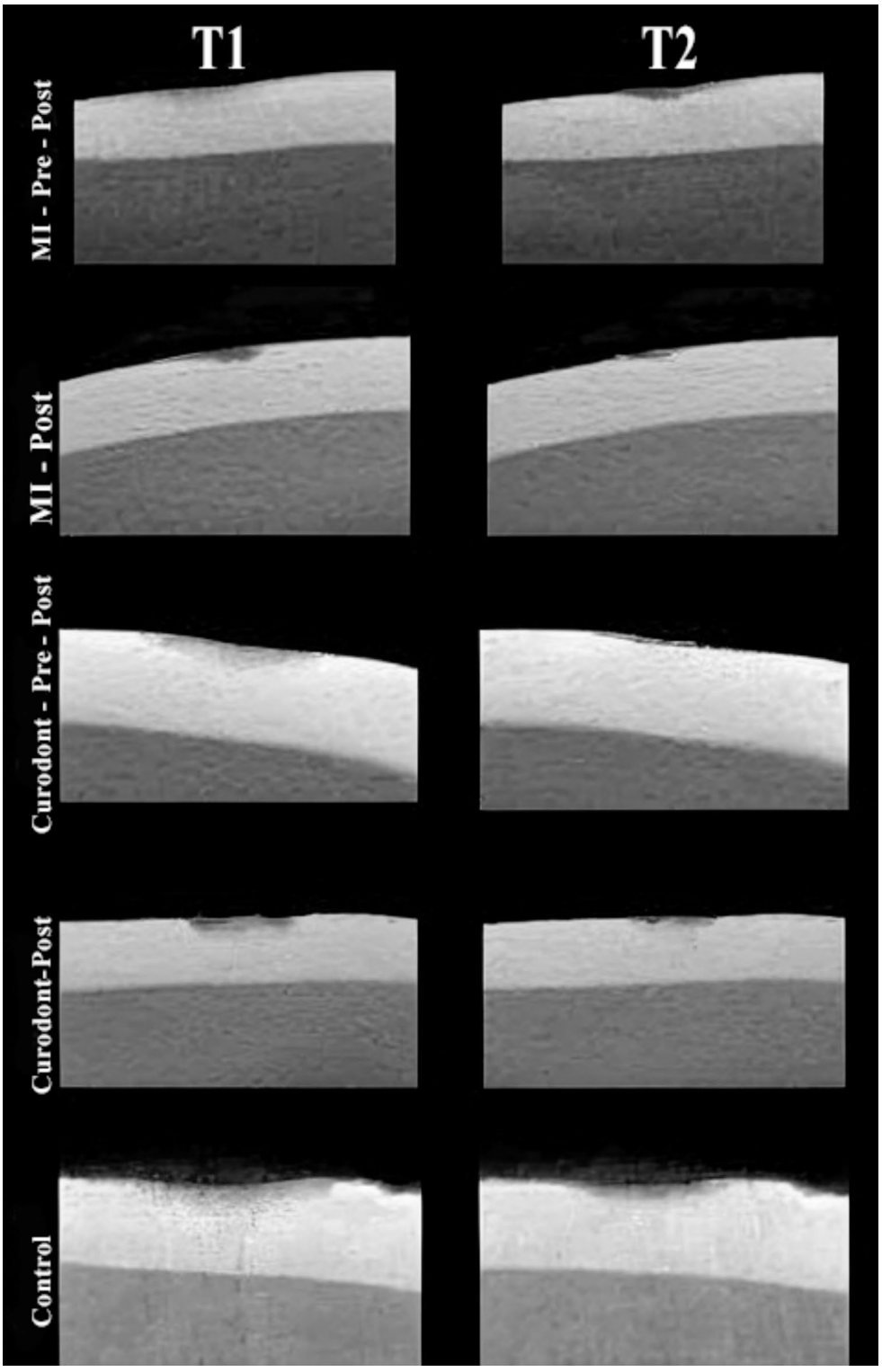

Fig. 2. Micro-CT images obtained after demineralization (T1) and remineralization (T2). *MI-Pre-Post* MI varnish applied before and after demineralization, *MI-Post* MI varnish applied after demineralization, *Curodont-Pre-Post* Curodont FP applied before and after demineralization, *Curodont-Post* Curodont FP applied after demineralization, *Control* No remineralization agent applied after demineralization (kept in saliva).

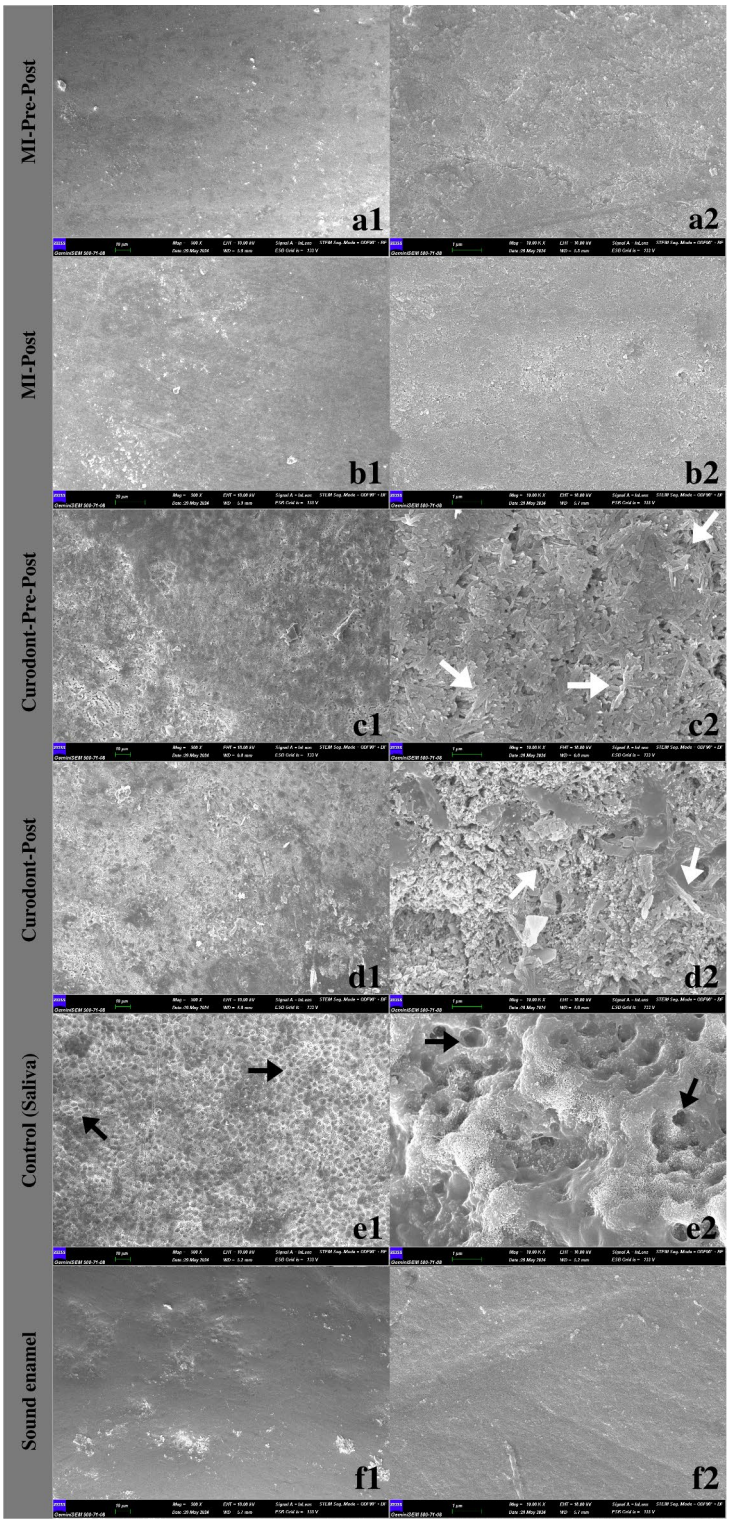

Fig. 3. SEM images of specimen surfaces of the experimental and control groups after 28 days. (**a1**), (**b1**), (**c1**), (**d1**), (**e1**), (**f1**) show the enamel surface under 500x magnification. (**a2**), (**b2**), (**c2**), (**d2**), (**e2**), (**f2**) show the enamel surface under 10.000x magnification.

measurements, this study assessed enamel density solely through ultrasonic velocity analysis and concluded that the specimens were unaffected by demineralization, based on SEM images. An enamel is a mineralized tissue with a highly complex hierarchical structure composed of enamel rods arranged perpendicular to the tooth surface. The orientation of enamel prisms can influence ultrasonic velocity readings[31]. Therefore micro-CT offers more accurate and objective results for assessing mineral density.

	Ca	P	Ca/P
MI-pre-post	45.97 ± 1.40 [a]	19.87 ± 0.07 [a]	2.31 ± 0.06[ac]
MI-post	41.51 ± 2.25 [ab]	19.01 ± 0.82 [ab]	2.18 ± 0.02[bc]
Curodont- pre-post	42.030 ± 1.18 [ab]	17.84 ± 0.40 [b]	2.36 ± 0.05[a]
Curodont-post	40.53 ± 0.76 [ab]	17.43 ± 0.01 [b]	2.33 ± 0.04[a]
Control	39.91 ± 1.93 [b]	18.38 ± 0.64 [ab]	2.17 ± 0.05[b]
Sound enamel	41.00 ± 5.01 [ab]	18.96 ± 1.36 [ab]	2.16 ± 0.11[b]
Test stat.	2.969	721.716	8.854
p-value	**0.040**	**< 0.001**	**< 0.001**

Table 4. Mean Ca and P elemental composition values (wt %) and standard deviation values of the groups. Note: Elemental composition values are based on the the One-way ANOVA test. [a–c]: No difference between groups with the same letter for each measurement for Ca, P and Ca/P. p-values presented in bold font indicate statistical significance ($p < 0.05$). *MI-Pre-Post* MI varnish applied before and after demineralization, *MI-Post* MI varnish applied after demineralization, *Curodont-Pre-Post* Curodont FP applied before and after demineralization,*Curodont-Post* Curodont FP applied after demineralization, *Control* No remineralization agent applied after demineralization (kept in saliva), *T0* baseline micro-CT imaging, *T1* Micro-CT imaging following demineralization, *T2* Micro-CT imaging after experimental period (28 days)

SAP P11-4 has been reported to bind to calcium ions[12,22,23]. However, it is hypothesized that SAP P11-4 might also prevent the initiation of WSLs by binding to sound enamel owing to its calcium-binding capacity[32]. For a cariostatic agent to effectively exert its protective effects in clinical settings, such as positively influencing the balance between demineralization and remineralization, or inhibiting bacterial biofilm formation, it is crucial that the agent can adequately bind to the enamel[32]. In a recent study, EDX analysis of the enamel surface following the application of Curodont to sound bovine teeth did not detect any traces of the self-peptide on the enamel[32]. Although the pH cycling model was used in this study, it is hypothesized that the protective efficacy of the self-peptide is lower than that of fluoride owing to insufficient adhesion to the intact enamel surface. This hypothesis is supported by our study, which concluded that the calcium-binding capacity of Curodont FP is not sufficient to ensure effective binding to the sound enamel surface.

Studies on fluoride varnishes indicate that their effectiveness against acidic attacks is not solely attributed to their high fluoride concentrations but also to their prolonged adhesion to the enamel surface[32,33]. MI Varnish, for instance, enhances surface resistance by forming calcium fluoride on the enamel, providing a fluoride reserve that mitigates demineralization[34]. Unlike other fluoride varnishes, MI Varnish also inhibits demineralization by forming 'amorphous calcium phosphate (ACP) crystals' and 'apatite' on the enamel surface. The high affinity of ACP for fluoride enables the release of nearly four times more fluoride into the oral environment than conventional fluoride varnishes. ACP effectively inhibits enamel and dentin demineralization by stabilizing calcium and phosphate ions in the saliva, thereby preventing demineralization and promoting remineralization. When adequate amounts of calcium and phosphate ions are available, fluoride ions can facilitate the remineralization of enamel lesions and precipitate new mineral formation[34,35]. CPP-ACP, when present in enamel subsurface lesions, releases weakly bound calcium and phosphate ions with high binding affinity with apatite[36]. Consistent with this, the present study findings concluded that the application of MI varnish on sound enamel significantly inhibited the formation of WSL by effectively preventing mineral density loss in a low pH environment, compared to both the control group and the Curodont FP group.

The second aspect examined in the present study was a comparative evaluation of the remineralization efficacy of Curodont FP, MI varnish, and saliva. As expected, following the application of Curodont FP or MI varnish to WSL, a significant reduction in the volume, area, and depth of WSL was observed, accompanied by a notable increase in enamel mineral density. The changes observed in the control group samples from baseline to day 28 suggest that some degree of natural remineralization occurred in the WSL. In some in vitro studies[15,37,38], artificial saliva solution, commonly used as a negative control, has been reported to have remineralization potential for WSL. However, according to the results of our current study, while artificial saliva exhibits some remineralization potential, the increase in mineral density observed after demineralization and subsequent remineralization was not statistically significant and was substantially lower than that in the agent-treated groups. Thus, it should be noted that the remineralization effect of saliva was limited, and natural remineralization was not observed in some specimens within this negative control group. These results suggest that artificial saliva is only effective in preventing the progression of incipient carious lesions rather than effectively curing them. However, it should not be ruled out that artificial saliva may have the potential to reduce WSL in long-term studies, and further research could be conducted to explore its effectiveness in this context.

The remineralization activity of the MI varnish group was significantly higher than that of the control group, supporting the findings of previous studies[15,18–20,39,40]. The reason for preferring MI varnish in our study was the conclusion in the literature that CPP-ACPF application demonstrated greater effectiveness than fluoride alone[13,41,42]. It has been reported that MI varnish enhances the stability of calcium and phosphate ions on the demineralized enamel surface owing to its CPP-ACP content[15]. Similarly, the remineralization activity of the Curodont group was significantly higher than that of the control group, which is similar to the results of previous studies[15,38,40]. In our recent study using an in vitro pH cycle model, we demonstrated that the $P_{11\text{-}4}$ peptide fibers enhanced the remineralization of WSL and facilitated hydroxyapatite formation. This process initially led to

surface remineralization with the development of needle-shaped crystals, followed by an increase in mineral density and remineralization of subsurface lesions. Self-assembling peptides represent an innovative approach that naturally aids in the integration of calcium and phosphate from saliva, thereby promoting the formation of an enamel matrix[15]. Therefore, we propose that the observed effect of self-assembling peptides in promoting enamel remineralization could have potential clinical utility.

The Curodont FP group demonstrated a greater increase in mineral density between the T1 and T2 time periods than the MI Varnish group. Several studies assessing the remineralization activity of fluoride-containing agents have recommended Curodont for its potential to enhance mineral gain and prevent mineral loss, highlighting its superior efficacy[15,39,43,44]. The ability of self-peptides to form scaffold-like structures with negatively charged sites plays a key role in regulating the initial mineral deposition and promoting subsequent hydroxyapatite crystal growth[21]. Therefore, the presence of self-peptide following demineralization may facilitate a rapid return to initial mineral concentrations, thereby enabling immediate remineralization of the enamel substrate[31]. Self-assembling peptides are thought to penetrate the subsurface layer and are more effective in addressing subsurface lesions[45]. Welk et al.[45]. demonstrated the effect of P_{11-4} on carious lesions induced by orthodontic treatment using multiple brackets. The authors concluded that treating initial carious lesions with P_{11-4} resulted in superior remineralization of subsurface lesions compared to that in control teeth. However, in this study, the impedance method and morphometric measurements were also performed using the Shadepilot, which may not be sufficient to assess subsurface efficacy. Although Curodont FP increased mineral density more than MI Varnish, no significant difference in lesion depth was observed between the two treatments in the present study. This may be attributed to the fluoride varnish used in our study, which not only contains NaF, but also CPP-ACP, a compound (CPP-ACPF) that demonstrates superior remineralization properties compared to traditional fluoride varnishes[13,15]. CPP-ACP-containing agents have demonstrated the ability to penetrate the subsurface areas of incipient enamel caries by serving as reservoirs of calcium and phosphate ions, thereby facilitating remineralization[14,19]. Another possible reason for this could be the fluoride content in Curodont FP. Fluoride in its composition may have caused a significant increase in the surface enamel density, potentially reducing the effectiveness of the peptide in the subsurface region.

In the present study, a period of 28 days was used to evaluate the remineralization of WSL lesions. Following the application of the remineralization agents, the samples were subjected to pH cycling throughout the experimental period to simulate the oral environment. In in vitro studies investigating the remineralization of WSL, varying durations, such as 5, 7, 15, 28, or 30 days, have been reported[29,43,46,47]. In the literature, the clinical remineralization effect of both fluoride-containing agents and self-assembling peptides has been reported with applications lasting 28 days or longer[21,48]. In order to allow a more comprehensive evaluation of the remineralization process in both superficial and deeper layers, a period of 4 weeks (28 days) was chosen in our study.

The demineralization and remineralization processes on enamel are challenging to detect in the early stages through visual inspection alone. Researchers have noted that micro-CT, as an alternative to the histological section method, which is regarded as the gold standard, demonstrates a high correlation with this method and offers greater sensitivity for in vitro conditions[49]. The advantages of this system include the absence of the need for sample preparation, the ability to perform repeated scans without damaging the lesion, the capability to evaluate the lesion in 3D, and the production of highly sensitive results[47]. Therefore, the micro-CT system was preferred to evaluate the changes in depth, surface area, volume, and density of the WSLs in this study.

In the present study, EDX, a widely recognized method for determining the mineral content of dental hard tissues, was employed to assess the impact of various remineralization agents on the calcium (Ca) and phosphorus (P) contents of enamel surfaces. The Ca/P ratio in the sound enamel group, which served as the negative control, was 2.16, which was higher than that reported in the literature[33,50,51]. This variation may be attributed to differences in the specific experimental conditions or age ranges of the bovine specimens. MI varnish, particularly with a single application, did not elevate the Ca/P ratio as effectively as did Curodont FP. Curodont FP, used in the current study, contains 0.05% oligopeptides. A further increase in the Ca/P ratio can be attributed to the synergistic effect of these two remineralization agents. The EDX analysis results of this study are consistent with the findings of Yaşar et al.[29], who evaluated the remineralization efficacy of a novel biomimetic remineralization agent, peptide, and fluoride gel in permanent human molars. They reported that fluoride gel exhibited a lower Ca/P ratio than both the peptide and peptide + fluoride groups. However, in a study on bovine incisors, the initial surface accumulation of cerium and oligopeptide P_{11-4} was compared with that of fluoride for caries prevention[32]. They reported that the Ca/P ratio in the fluoride groups [NaF and AmF (Amine Flouride)] was higher than that in the control and oligopeptide P_{11-4} groups. It was suggested that this was due to the insufficient calcium-binding capacity of oligopeptide P_{11-4}, which may not have been strong enough to effectively bind to the intact enamel surface. However, in the current study, it was found that the Ca/P ratio in groups treated with Curodont FP, whether applied pre-post or post demineralization, was significantly higher than that in the group treated with MI Varnish post demineralization. This result aligns with the established properties of Curodont FP, which penetrates demineralized enamel micropores, forms a scaffold, and enhances the deposition of calcium and phosphate ions from saliva, thereby increasing the overall mineral content of enamel.

The present study demonstrated that both MI Varnish and Curodont FP halted the progression of WSL and promoted remineralization. MI Varnish showed superior efficacy in preventing demineralization, whereas self-assembling peptides exhibited enhanced remineralization potential compared to fluoride varnishes. These findings indicate that both agents possess promising remineralization capabilities; however, further research under in vivo conditions is necessary to validate these results.

The use of bovine teeth in this study could be considered a limitation, as differences in genetic and environmental factors between bovine and human enamel may have affected the results. However, the preference for bovine

incisors in this study is attributed to their greater accessibility, superior preservation, uniform structure, and ability to prepare multiple samples from a single tooth because of their larger dimensions[38]. The present study was conducted in vitro and may have limited applicability in clinical practice, as it does not accurately reflect actual oral conditions and patient compliance. The short-term effects of these agents limit the generalizability of the results obtained, suggesting the need for comprehensive and long-term studies to evaluate the long-term efficacy of different remineralization agents. Future research should focus on in vivo validation to determine the clinical efficacy of these agents under real intraoral conditions. In addition, the evaluation of diverse application protocols and examination of the combination of remineralization agents with additional strategies, such as bioactive materials or probiotic therapies, has the potential to enhance the effectiveness of treatment approaches.

Conclusions

Effective clinical management is crucial to protect intact enamel from demineralization, especially before treating WSLs. The application of MI Varnish can improve enamel resistance to acid attacks and prevent demineralization in high-risk patients, particularly before orthodontic treatment. Both the MI Varnish and Curodont FP showed significant efficacy in remineralizing early carious lesions. However, further in vitro and in vivo studies with varied materials and longer observation periods are required to validate and refine these findings.

Data availability

Data supporting the findings of this study are available from the corresponding author upon request.

Received: 8 January 2025; Accepted: 24 March 2025
Published online: 03 April 2025

References

1. Sharab, L. et al. Effect of patients' attitude and perception of oral hygiene on white spot lesion development and plaque accumulation during orthodontic treatment: A survey of patients with fixed appliances. *J. Orofac. Orthop.* **85**, 34–40 (2024).
2. Salerno, C. et al. Distribution of initial caries lesions in relation to fixed orthodontic therapy. A systematic review and meta-analysis. *Eur. J. Orthod.* **46**, 1–15 (2024).
3. Zeidan, N. K., Enany, N. M., Mohamed, G. G. & Marzouk, E. S. The antibacterial effect of silver, zinc-oxide and combination of silver/zinc oxide nanoparticles coating of orthodontic brackets (an in vitro study). *BMC Oral Health.* **22**, 230 (2022).
4. Chen, I. et al. Alterations in subgingival microbiota during full-fixed appliance orthodontic treatment—A prospective study. *Orthod. Craniofac. Res.* **25**, 260–268 (2022).
5. Wierichs, R. J., Carvalho, T. S. & Wolf, T. G. Efficacy of a self-assembling peptide to remineralize initial caries lesions-A systematic review and meta-analysis. *J. Dent.* **109**, 103652 (2021).
6. Xie, Z., Yu, L., Li, S., Li, J. & Liu, Y. Comparison of therapies of white spot lesions: a systematic review and network meta-analysis. *BMC Oral Health.* **23**, 346 (2023).
7. Hussain, U. et al. Prevalence, incidence and risk factors of white spot lesions associated with orthodontic treatment–A systematic review and meta-analysis. *Orthod. Craniofac. Res.* https://doi.org/10.1111/ocr.12888 (2025).
8. Sardana, D., Schwendicke, F., Kosan, E. & Tüfekçi, E. White spot lesions in orthodontics: consensus statements for prevention and management. *Angle Orthod.* **93**, 621–628 (2023).
9. Shetty, S. S. & Nekkanti, S. Remineralization potential of a novel biomimetic material (Self-assembling peptide P_{11-4}) on early enamel caries: an *In vitro* study. *J. Contemp. Dent. Pract.* **24**, 182 (2023).
10. Chan, A. K. Y. et al. Clinical evidence for professionally applied fluoride therapy to prevent and arrest dental caries in older adults: A systematic review. *J. Dent.* **125**, 104273 (2022).
11. Shah, M. et al. Comparative assessment of conventional and light-curable fluoride varnish in the prevention of enamel demineralization during fixed appliance therapy: a split-mouth randomized controlled trial. *Eur. J. Orthod.* **40**, 132–139 (2018).
12. Bröseler, F. et al. Randomised clinical trial investigating self-assembling peptide P 11 – 4 in the treatment of early caries. *Clin. Oral Investig.* **24**, 123–132 (2020).
13. Beigoli, S., Sabouri, Z., Moghaddas, S. S. T. H., Heydari, A. & Darroudi, M. Exploring the biophysical properties, synergistic antibacterial activity, and cell viability of nanocomposites containing casein phosphopeptides and amorphous calcium phosphate. *J. Drug Deliv Sci. Technol.* **86**, 104680 (2023).
14. Giacaman, R. A., Maturana, C. A., Molina, J., Volgenant, C. & Fernández, C. E. Effect of casein phosphopeptide-amorphous calcium phosphate added to milk, chewing gum, and candy on dental caries: a systematic review. *Caries Res.* **57**, 106–118 (2023).
15. Üstün, N. & Aktören, O. Analysis of efficacy of the self-assembling peptide-based remineralization agent on artificial enamel lesions. *Microsc. Res. Tech.* **82**, 1065–1072 (2019).
16. Llena, C., Leyda, A., Forner, L. & CPP-ACP CPP-ACFP versus fluoride varnish in remineralisation of early caries lesions. A prospective study. *Eur. J. Paediatr. Dent.* **16**, 181–186 (2015).
17. Kilic, M. & Gurbuz, T. Evaluation of the effects of different remineralisation agents on initial enamel lesions by scanning electron microscope and energy-distributed X-ray analysis. *Int. J. Clin. Pract.* **75**, e14299 (2021).
18. Yan, J., Yang, H., Luo, T., Hua, F. & He, H. Application of amorphous calcium phosphate agents in the prevention and treatment of enamel demineralization. *Front. Bioeng. Biotechnol.* **10**, 853436 (2022). (2022).
19. Gore, A. B., Patel, S. P., Gulve, M. N. & Aher, G. B. Comparative evaluation of the remineralizing potential of different calcium and fluoride-based delivery systems on artificially demineralized enamel surface; an in vitro study. *J. Conservative Dentistry Endodontics.* **25**, 292–296 (2022).
20. Yazicioğlu, O., Yaman, B. C., Güler, A. & Koray, F. Quantitative evaluation of the enamel caries which were treated with casein phosphopeptide-amorphous calcium fluoride phosphate. *Niger J. Clin. Prac.* **20**, 686–692 (2017).
21. Brunton, P. A. et al. Treatment of early caries lesions using biomimetic self-assembling peptides–a clinical safety trial. *Br. Dent. J.* **215**, E6–E6 (2013).
22. Kind, L. et al. Biomimetic remineralization of carious lesions by self-assembling peptide. *J. Dent. Res.* **96**, 790–797 (2017).
23. Dawasaz, A. A., Togoo, R. A., Mahmood, Z. & Azlina, A. Thirumulu Ponnuraj, K. Effectiveness of self-assembling peptide (P11-4) in dental hard tissue conditions: A comprehensive review. *Polymers* **14**, 792 (2022).
24. Amin, O. A., Shaalan, O. O. & Riad, M. Remineralization potential of curodont repair Flouride plus versus CPP-ACP in white spot lesions. *J. Adv. Dent.* **5**, 110–118 (2023).
25. Hong, S-C., Lee, D-Y. & Kim, Y-J. Micro-computed tomographic evaluation of the effect of fluoride agents on white spot lesions: an in vitro study. *Korean J. Orthod.* **52**, 75–79 (2022).
26. de Mello Vieira, A. E. et al. Fluoride dose response in pH-cycling models using bovine enamel. *Caries Res.* **39**, 514–520 (2005).

27. Buskes, J., Christoffersen, J. & Arends, J. Lesion formation and lesion remineralization in enamel under constant composition conditions: a new technique with applications. *Caries Res.* **19**, 490–496 (1985).
28. Klimek, J., Hellwig, E. & Ahrens, G. Fluoride taken up by plaque, by the underlying enamel and by clean enamel from three fluoride compounds in vitro. *Caries Res.* **16**, 156–161 (1982).
29. Yaşar, M., Bal, C., Aksoy, M., Güngörmüş, M. & Orhan, K. In vitro caries-preventive effect of a mineralization-promoting peptide combined with fluoride gel on sound primary teeth. *Int. J. Paediatr. Dent.* **34**, 256–266 (2024).
30. Feldkamp, L. A. Practical cone beam algorithm. *J. Microsc.* **185**, 67–75 (1997).
31. Takahashi, F. et al. Ultrasonic assessment of the effects of self-assembling peptide scaffolds on preventing enamel demineralization. *Acta Odontol. Scand.* **74**, 142–147 (2016).
32. Scholz, K. J. et al. Surface accumulation of Cerium, Self-Assembling peptide, and fluoride on sound bovine enamel. *Bioeng* **9**, 760 (2022).
33. Comar, L. P. et al. Mechanism of action of TiF4 on dental enamel surface: SEM/EDX, KOH-soluble F, and X-ray diffraction analysis. *Caries Res.* **51**, 554–567 (2018).
34. Shetty, R. S., Bhat, S. S., Hegde, S. K. & Bhat, V. S. Effect of Fluoride-based varnishes with added calcium and phosphate on microhardness of esthetic restorative materials: an in vitro study. *Int. J. Clin. Pediatr. Dent.* **15**, 187–193 (2022).
35. Salem, M. N., Gohar, R. A., Hafez, S. I. & Abulnoor, B. A. Classical versus non-classical strategies for remineralization of early enamel lesions: systematic review and meta-analysis. *J. Int. Oral Health.* **13**, 214–226 (2021).
36. Nakata, T., Kitasako, Y., Sadr, A., Nakashima, S. & Tagami, J. Effect of a calcium phosphate and fluoride paste on prevention of enamel demineralization. *Dent. Mater. J.* **37**, 65–70 (2018).
37. Enax, J., Fandrich, P., Schulze zur Wiesche, E. & Epple, M. The remineralization of enamel from saliva: A chemical perspective. *Dentistry J.* **12**, 339 (2024).
38. Lena Sezici, Y., Yetkiner, E., Aykut Yetkiner, A., Eden, E. & Attin, R. Comparative evaluation of fluoride varnishes, self-assembling peptide-based remineralization agent, and enamel matrix protein derivative on artificial enamel remineralization in vitro. *Prog Orthod.* **22**, 1–12 (2021).
39. Alkilzy, M., Santamaria, R., Schmoeckel, J. & Splieth, C. H. Treatment of carious lesions using self-assembling peptides. *Adv. Dent. Res.* **29**, 42–47 (2018).
40. Memarpour, M., Razmjouei, F., Rafiee, A. & Vossoughi, M. Remineralization effects of self-assembling peptide P11-4 associated with three materials on early enamel carious lesions: an in vitro study. *Microsc. Res. Tech.* **85**, 630–640 (2022).
41. Dai, Z. et al. Effects of fluoride and calcium phosphate materials on remineralization of mild and severe white spot lesions. *Biomed Res Int.* 1271523 (2019). (2019).
42. Shen, P. et al. Remineralization and fluoride uptake of white spot lesions under dental varnishes. *Aust Dent. J.* **65**, 278–285 (2020).
43. Jablonski-Momeni, A., Nothelfer, R., Morawietz, M., Kiesow, A. & Korbmacher-Steiner, H. Impact of self-assembling peptides in remineralisation of artificial early enamel lesions adjacent to orthodontic brackets. *Sci. Rep.* **10**, 15132 (2020).
44. Schmidlin, P., Zobrist, K., Attin, T. & Wegehaupt, F. In vitro re-hardening of artificial enamel caries lesions using enamel matrix proteins or self-assembling peptides. *J. Appl. Oral Sci.* **24**, 31–36 (2016).
45. Welk, A., Ratzmann, A., Reich, M., Krey, K. & Schwahn, C. Effect of self-assembling peptide P11-4 on orthodontic treatment-induced carious lesions. *Sci. Rep.* **10**, 6819 (2020).
46. Özdemir, Ş., Taran, P. K., Mammadlı, N., Altınova, İ. S. & Gazioğlu, I. Remineralization potential of P11-4 and fluoride on secondary carious primary enamel: A quantitative evaluation using microcomputed tomography. *Microsc Res. Tech.* **85**, 807–812 (2022).
47. Kucuk, E. B., Malkoc, S. & Demir, A. Microcomputed tomography evaluation of white spot lesion remineralization with various procedures. *Am. J. Orthod. Dentofac. Orthop.* **150**, 483–490 (2016).
48. Sivapriya, E., Sridevi, K., Periasamy, R., Lakshminarayanan, L. & Pradeepkumar, A. R. Remineralization ability of sodium fluoride on the microhardness of enamel, dentin, and dentinoenamel junction: an: in vitro: study. *J. Conserv. Dent.* **20**, 100–104 (2017).
49. Özkan, G., Kanli, A., Başeren, N. M., Arslan, U. & Tatar, İ. Validation of micro-computed tomography for occlusal caries detection: an in vitro study. *Braz Oral Res.* **29**, 01–07 (2015).
50. Möhring, S. et al. Elemental compositions of enamel or dentin in human and bovine teeth differ from murine teeth. *Mater* **16**, 1514 (2023).
51. Silva Soares, L. E. & do Espírito Santo, A. M. Morphological and chemical comparative analysis of the human and bovine dentin–adhesive layer. *Microsc Microanal.* **21**, 204–213 (2015).

Acknowledgements
The authors would like to express their gratitude to Assoc. Prof. Dr. Naci Murat for his invaluable assistance during the statistical analysis. The authors would also like to acknowledge the support of Assoc. Prof. Dr. Arda Büyüksungur from Ankara University in conducting micro-CT imaging.

Author contributions
"H.D contributed to conceptualization, methodology, investigation, formal analysis, manuscript review and editing and original draft preparation; E.D contributed to investigation, formal analysis and manuscript review and editing; K.O contributed to micro-ct analysis."

Funding
This work was supported by the Research Fund of Nuh Naci Yazgan University [grant numbers 2023-SA.DH.BP/25].

Declarations

Competing interests
The authors declare no competing interests.

Ethics approval
This study was performed in line with the principles of the Declarations of Helsinki. The study protocol was approved by Clinical Research Ethics Committee of Nuh Naci Yazgan University where the study was contucted (no. 2023/003–004).

Additional information

Correspondence and requests for materials should be addressed to H.D.

Reprints and permissions information is available at www.nature.com/reprints.

Publisher's note Springer Nature remains neutral with regard to jurisdictional claims in published maps and institutional affiliations.